Pertanika J. Sci. & Technol. 30 (2): 1237 - 1256 (2022)

PERTANIKA JOURNALS

SCIENCE & TECHNOLOGY

Journal homepage: http://www.pertanika.upm.edu.my/

Electrophoretic Deposition of Hexagonal Boron Nitride Particles from Low Conductivity Suspension

Kok-Tee Lau* and Shahrizal Samsudin

Faculty of Mechanical and Manufacturing Engineering Technology, Universiti Teknikal Malaysia Melaka, Hang Tuah Jaya, 76100 Durian Tunggal, Melaka, Malaysia

ABSTRACT

Given that hexagonal boron nitride (hBN) particles are extremely stable in colloidal suspensions due to their low density, they are difficult to deposit via electrophoretic deposition (EPD). Poly (diallyldimethylammonium chloride) (PDDA) is widely used as a polyelectrolyte for ceramic particles because of its strong electrophoretic response. Nevertheless, studies on PDDA as a functionalising agent of hBN particles for EPD remain elusive. Here, hBN particles were functionalised with different amounts of PDDA to investigate effects on suspension stability and EPD yield. Deionised (DI)-water-based hBN particle suspensions with PDDA contents that varied from 0.3 wt% and 0.6 wt% (of hBN basis) were prepared using washed as-received hBN particles. Then, washed and nonwashed PDDA-functionalised hBN particle groups were prepared by subjecting only the former to water washing. Washing, which involved the repeated particle dispersion in DI water and vacuum filtration, successfully reduced the conductivity of the aqueous hBN suspension to 2 μS/cm, which was significantly lower than the conductivities of ~180 and ~25 μS/cm shown by the as-received particle suspension and PDDA-functionalised particles before washing. This result indicated that washing eliminated the interference of free ions on the suspension stability of hBN particles and EPD yield. In contrast to that of the nonwashed group, the suspension stability of the washed group decreased as the PDDA content was increased. Nevertheless, at 0.3 wt% and 0.6 wt% PDDA, the EPD yields of the washed group were 183% to 31% higher than those of the nonwashed group. This study provided new insight into the EPD of hBN particles using low-cost aqueous suspensions with sustainable ultralow ion conductivity.

Keywords: Aqueous suspension, colloidal particles, electrophoretic deposition, functionalisation, hexagonal boron nitride, ion conductivity, poly (diallyldimethylammonium chloride), water washing

ARTICLE INFO

Article history:
Received: 28 August 2021
Accepted: 15 December 2021
Published: 11 March 2022

DOI: https://doi.org/10.47836/pjst.30.2.21

E-mail addresses:
ktlau@utem.edu.my (Kok-Tee Lau)
rizalsamdally@gmail.com (Shahrizal Samsudin)
*Corresponding author

ISSN: 0128-7680
e-ISSN: 2231-8526

INTRODUCTION

Hexagonal boron nitride (hBN) has potential applications as a thermal and electrical isolation interface material because of its high thermal conductivity and dielectric strength. The rare combination of both properties makes hBN material a promising candidate for the next-generation thermal management material of semiconductor packages. Recent studies have combined hBN particles (i.e., as a filler) with commercially available polymer matrices through various preparation methods (Khalaj et al., 2020; Yu et al., 2021). The applications of hBN in water treatment, energy storage, solar cells, carbon capture and catalysis, have also been explored by utilising hBN in the form of free particles or deposited as coatings (Hafeez et al., 2020; Ihsanullah, 2020). hBN particles are typically surface modified to improve their integration with other materials. The surface functionalisation of hBN particles with a functionalising agent is considered a facile approach to achieving this objective.

Poly (diallyldimethylammonium chloride) (PDDA) is widely used as a polycation for the functionalisation of ceramic particles and polymer fibres because of its strong electrostatic adsorption with other materials (Cui et al., 2021; Du et al., 2020; Muto et al., 2020; Nasser et al., 2020). Nevertheless, studies on functionalisation with PDDA as a fixation agent or a flocculant of hBN particles for electrophoretic interaction in electrophoretic deposition (EPD)remain elusive. hBN particles are extremely stable in the form of colloidal suspension particles because of their low density and are thus difficult to deposit on a targeted substrate via EPD in the absence of a flocculant (Narayanasamy et al., 2016). Furthermore, recent publications on PDDA usage for the EPD of other types of particles did not mention or discuss the possible EPD yield problem caused by ion impurities originating from suspension particles and by PDDA addition (Katagiri et al., 2018; Lalau & Low, 2019; Lin et al., 2016; Sanchez et al., 2021). EPD yield remains limited by the detrimental change in the ion conductivity of EPD suspensions from time zero, especially when the EPD time exceeds 10 min (Tiwari et al., 2020).

Water washing has been very effective in removing water-soluble ions from contaminated ceramic particles, particularly when combined with mechanical agitation and properly controlled washing parameters (Bandara et al., 2020; Gautam et al., 2020). Although water washing has long been practised in the purification of as-received hBN particles, the water washing of PDDA-functionalised hBN particles has not been reported. The previous study showed that the high suspension stability of hBN particles limits EPD yields (Narayanasamy et al., 2016). Thus, adjusting ion concentrations (or pH) using electrolytes or polyelectrolytesis necessary to achieve suspension stability and increase deposition yield. However, considerably high electrolyte or polyelectrolyte concentrations during EPD contribute to the gradual but progressive electrolytic corrosion on the counter electrode and disturb the chemical equilibriumof EPD suspensions (Lau & Sorrell, 2013). Thus, the ion

impurities of the as-received hBN particles and excess PDDA (which does not attach onto the surfaces of hBN particles after PDDA functionalisation) must be minimised during suspension preparation to ensure the optimal sustainability of EPD. The optimal EPD enables the deposition of a uniform hBN coating with sufficient thickness for the electrical isolation of thermal management components.

This work studied the effect of the repeated deionised (DI) water washing of PDDA-functionalised hBN particles on suspension stability and EPD yields. hBN particle agglomeration was highlighted given its necessity for understanding the relationship of sedimentation test data with EPD yields. However, this work did not discuss the control of particle agglomeration and the relationships with nanostructures because they were not the focus of the current study. Here, different amounts of PDDA were introduced into an aqueous hBN particle suspension to investigate the effect of PDDA addition on suspension stability and EPD yields. The facile water washing approach proposed here involved the repeated combination of DI water particle dispersion and vacuum filtration using an easily scaled-up equipment set. This study allowed the determination of new options for monitoring and improving EPD yields to enable the scaling up of EPD by potential manufacturing sectors.

MATERIALS AND METHOD

Materials Characteristics

hBN (99.8% purity, average particle = 0.6–1.2 μm) was supplied by Nova Scientific Resources (M) Sdn Bhd. The particles had well-rounded shapes and low sphericity (Figure 1). PDDA (CAS Number: 26062-79-3, average molecular weight M_W = 100 000–200 000, 20 wt% in H_2O) was supplied by Sigma–Aldrich (currently known as Millipore Sigma).

Polyscientific Enterprise Sdn. Bhd. supplied Reagent-grade DI water. Galvanised Iron (GI) sheet (commercial quality, thickness = 0.05 ± 0.004 cm) was supplied by Edutech Supply & Services (M) Sdn Bhd.

As-Received hBN Particle Washing Procedure

Firstly, 5 g of the as-received hBN particles were dispersed in 600 mL of DI water through agitation by an ultrasonic horn and magnetic stirring at medium settings for 15 min. The DI water was used straight from the packaged bottle. The particles were agitated under ambientenvironmental conditions to separate or dissolve the impurities of the as-received hBN particles into the water. The ion conductivity of the suspension before hBN particle washing was measured using a standard ion conductivity meter (Eutech PC 700). It was recordedas the ion conductivity of the control sample. Washing was performed for five cycles. Each cycle involved particle dispersion in fresh DI water followed by vacuum filtration with a filtration set (FAVORIT 40/38), which consisted of a receiver flask, a 300 mL glass funnel, hose connector and vacuum pump (ROCKER 2 motors). After each

washing cycle, the hBNparticles were collected in cake form using filter paper (1442-042, pore size = 2.5 µm, Whatman) and then dispersed and agitated again in fresh DI water. At the same time, the ionconductivity of the aqueous filtrate was recorded to monitor the washing performance. Finally, after the fifth vacuum filtration cycle, the filtered hBN particles were dried in a standard drying oven at 60°C for 30 min before use. The washing procedure is illustrated in Figure 2(i).

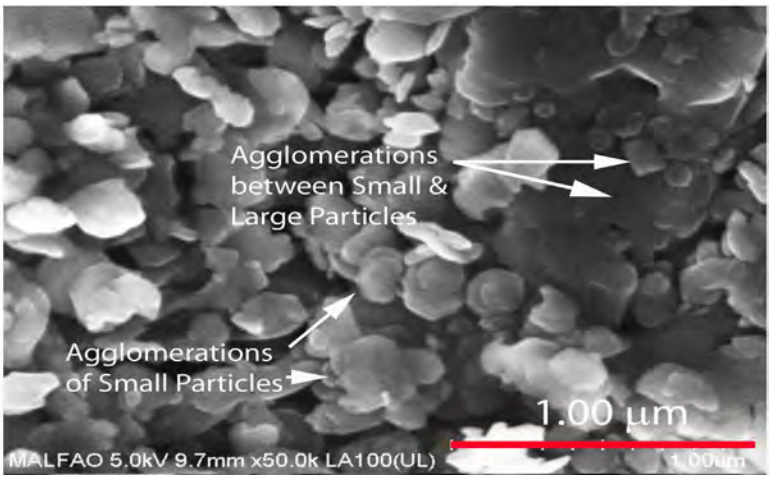

Figure 1. Surface microstructure of as-received hBN particles

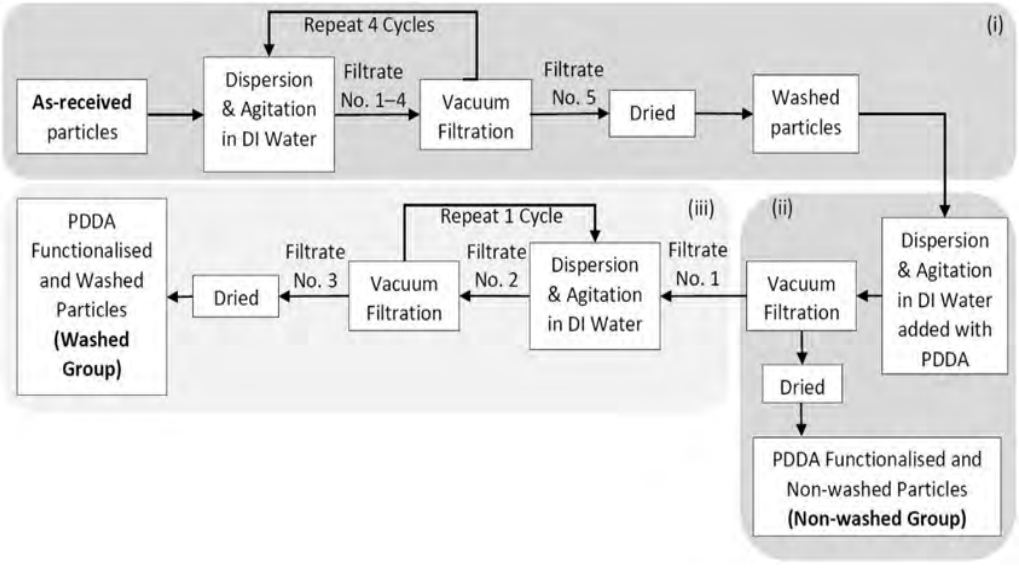

Figure 2. Schematic of the preparation of the (i) washed as-received, (ii) PDDA-functionalised and nonwashed particles and (iii) PDDA-functionalised and washed hBN particles. Filtrates that were collected during water washing were numbered in accordance with the collection sequence

hBN Particle Functionalisation and Preparation of Washed and Nonwashed Group hBN Particles

The washed as-received hBN particles were dispersed in DI water at the same solid loadings as those applied in the as-received hBN particle washing procedure. A controlled volume of PDDA solution was added during suspension agitation. Then, the functionalised particle suspension was washed and dried to remove the ion impurities introduced by functionalisation. Possible free ions included excess PDDAs, which were not attached to hBNparticles. In addition to conductivity, the pH of the aqueous filtrate from the washing process was recorded using Eutech PC 700 equipped with a standard pH probe. In the final stage, the four types of functionalised and washed hBN particles were added with 0.3 wt%, 0.4 wt%, 0.5 wt% and 0.6 wt% PDDA (the basis of hBN particle). The procedures are illustratedin Figures 2(ii) and 2(iii). The four samples were categorised as the washed group. The functionalised hBN particles that were collected from the filtration of the PDDA- functionalised h-BN particles immediately after functionalisation [Figure 2 (ii)] were categorised as the nonwashed group.

Particles Size Characterisation

The particles sizes of the as-received hBN particles before and after washing and washed hBN particles functionalised with 0.3 wt% PDDA were characterised using Malvern sizer2000. Approximately 1 g of particles was inserted into a sample measurement cell that contained distilled water as the dispersing medium. The particle suspension was ultrasonically agitated for 15 min before measurement.

Sedimentation Test Characterisation

Sedimentation tests were performed on the nonwashed and washed groups of the functionalised hBN particles to characterise particle suspension stability at different PDDA addition amounts. Each suspension sample was prepared by agitating 0.1 g of particles in 15 mL of DI water for 15 min and then immediately transferred into a screw-capped test tube. All the samples were vertically oriented and left undisturbed on a stable and horizontal table. Fourteen days after agitation, the sedimentation build-up (composed of opaque supernatant and sediment regions) of the samples was photographed, and the related heights were measured using a centimetre ruler. The suspension stability and sedimentation resultsfor the control sample that was not washed prior to functionalisation [Figure 2(i)] are shown as those for the 0 wt% sample (suspension of as-received particles) in the nonwashed group.

EPD Process and Deposition Yield Characterisation

For EPD, the solid loadings of functionalised hBN particle suspensions from the nonwashed and washed groups were prepared at the concentration of 1 mg/mL. A cathodic EPD was established using a DC power supply (Keysight E364xA) with a GI sheet (commercial grade, dimensions of 1.4 cm × 4 cm, thickness = 0.050 ± 0.004 cm) as the cathode and a titanium plate (99.9% purity, dimension = 1.6 × 3.5 × 0.2 cm) as the counter anode. The functionalised hBN particle suspension was agitated by magnetic stirring for 15 minutes and immediately used for EPD. EPD was performed at 60 V for 15 min using a vertical electrode set-up with an electrode separation of 1 cm and a GI sheet immersion depth of 1.70 ± 0.05 cm. The hBN-deposited GI sheets were then dried in an oven at 90 °C for 15 minbefore weighing. The deposition yield of hBN particles was obtained by subtracting the deposited GI weight from the blank GI weight.

Data collection was subjected to quality control during EPD. For each new EPD process, anew GI cathode was inserted, and the counter anode was rinsed with DI water and dried before insertion into a new suspension. The GI substrate was first polished, weighed and finally washed with acetone and DI water to remove the oxide layer and impurities. A newEPD suspension was freshly prepared using a similar method and instruments.

Raman Characterisation of hBN Deposit

The Raman spectra of hBN deposits were acquired via Raman spectroscopy (laser spot size =1 µm, exposure time = 1 s, accumulation = 10 times, 4 mW laser power, laser beam wavelength = 532 nm, solid-state laser, model: uniRAM-3500).

Microstructural Imaging of hBN Deposit

Images of the surface and cross-sectional microstructures of hBN deposits were captured using scanning electron microscopy (scanning electron mode, accelerating voltage = 30 kV,model: Evo 50, Carl Zeis AG).

Linear Fits of Sedimentation and Deposition Yield Data

The sedimentation and deposition yield data were linearly fitted with a linear regression model using MS Excel (Microsoft 365). All the fits showed R^2 values above 0.9. However, the sedimentation data of the nonwashed group had a low R^2 value of 0.1553.

RESULTS AND DISCUSSIONS

Ion Conductivity, pH and Particles Size Data

The electrical conductivities of the as-received hBN particle suspension and the filtrate obtained after the first wash were approximately 180 µS/cm [shown as Initial Conductivity

and data point for Filtrate No. 1 in Figure 3(a)], indicating the presence of a large concentration of dissolved ions. This work believed that the ions that had leached from the hBN particles contributed considerably to the filtrate's conductivity because the hBN particles could not pass through the filter given its pore size. Commercially available hBN particles contain considerable impurities after synthesis (Ertuğ, 2013). The synthesised hBN particles retained some unreacted residues even after undergoing purifications. The surfaces of BN materials have a strong tendency to adsorb contaminant ions because of thepresence of surface defects and ionic B–N bonds (Ihsanullah, 2020). This phenomenon suggests that impurities tend to exist on the manufactured hBN particles.

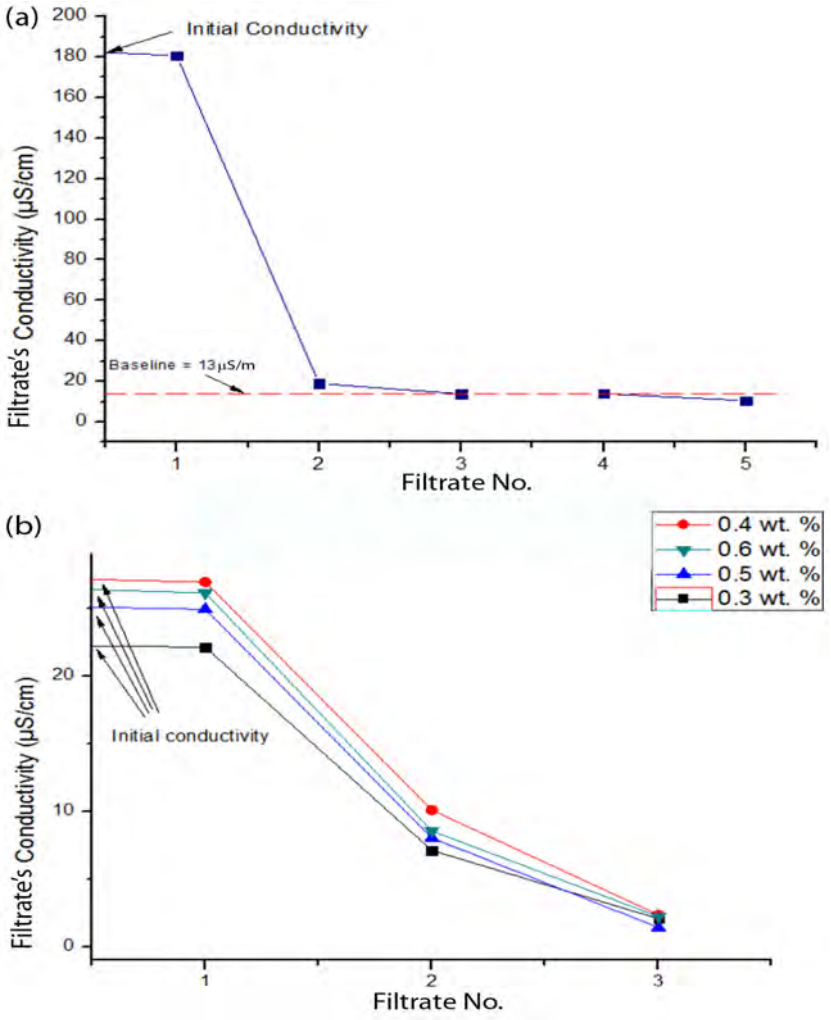

Figure 3. Ion conductivity of the filtrates obtained from the washing of (a) as-received hBN particles and (b) PDDA-functionalised hBN particles as a function of filtrate number

The filtrate collected from the second wash of the filtered hBN particles (labelled as Filtrate No. 2) had an extremely low conductivity (i.e., 19 µS/cm). This finding indicated that many ion impurities had been leached from the as-received hBN particles during the first wash. Nevertheless, the slight decrements in the conductivity of the filtrates from the third, fourth and fifth washes suggested that small amounts of ions were still being leached at a constant rate during these stages. The conductivity of the filtrate appeared to have plateaued at 13 µS/cm after the third wash. However, it was still relatively higher than the conductivity of fresh DI water, which is typically below 1 µS/cm (Li et al., 2020).

Figure 4(a) shows that the size range of the washed hBN particles remained within that of the as-received particles (between 0.3 and 24.7 µm) but had shifted towards small sizes (i.e., below 1.5 µm). The washed particles had a high-volume percentage of particles with sizes of 0.3–1.5 µm, whereas the as-received particles had a high-volume percentage of particles with sizes of 1.5–24.7 µm, before water washing, agglomerations formed amongst small particles and between small and large particles (Figure 1). Evidently, the water washing of the as-received hBN particles had reduced the percentage of the agglomerated particles and simultaneously reduced the percentage of large particles. Based on the particle size data, the deagglomeration of hBN particles continued with the subsequent water washing steps, thus gradually increasing the exposed surface area of hBN particles for ion dissolution. The extremely slow ion leaching due to deagglomeration accounted for the plateauing of the filtrate's conductivity at 13 µS/cm.

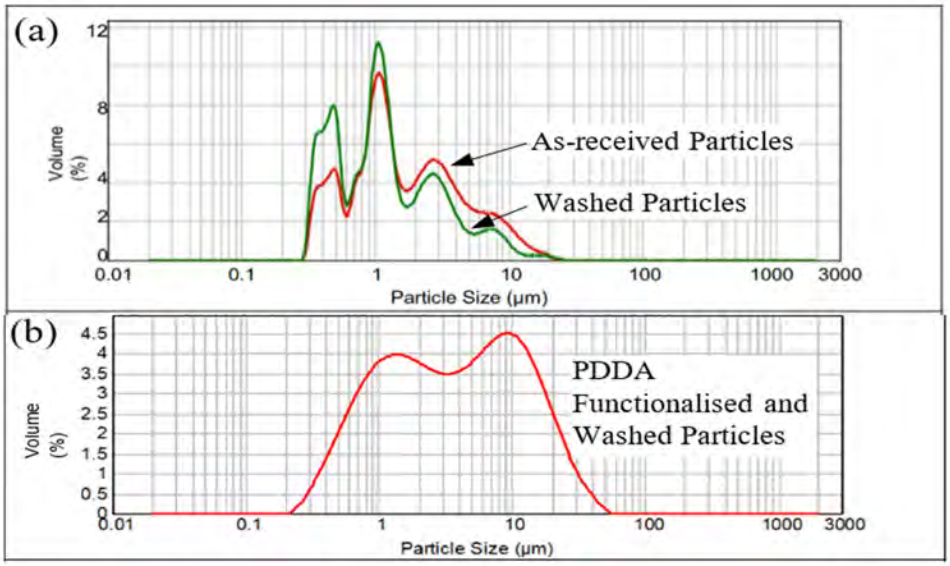

Figure 4. Particle size distributions of the (a) as-received hBN particles before and after water washing and (b) hBN particles functionalised with 0.3 wt% PDDA after water washing

The conductivity data of the washed as-received particles showed that three water washes removed more than 92% of the original ion impurities from the as-received hBN particles. Further washes did not significantly change the rate of ion impurity removal. Therefore, in this study, only three washes were used to remove the ion impurities introduced byPDDA functionalisation.

Figure 3(b) shows that all functionalised particle suspensions (i.e., 0.3 wt%, 0.4 wt%, 0.5 wt% and 0.6 wt% PDDA) exhibited similar conductivities with values of approximately 25.0 μS/m, which was 90% higher than the 13 μS/cm baseline displayed by the filtrate of the as-received hBN particles. The increase in conductivity was induced by the PDDA functionalisation of the hBN particles.

The conductivity of the filtrate obtained after the first wash (Filtrate No.1) was almost the same as that of the particle suspensions before filtering. This result implied that the conductivity of the filtrate was mainly contributed by the dissolved ions and not by the functionalised particles. The conductivity of the filtrate was two times higher than that of thefiltrate obtained after the fifth wash (i.e., 13 μS/m) of the as-received hBN particles, suggesting that PDDA functionalisation triggered further ion leaching from the hBN particles. Free PDDA molecules (unattached to particles) were unlikely to appear after the functionalisation of hBN particles because the conductivities measured during the washing of the functionalised particles did not vary significantly with the PDDA content (refer to Table 1).

Table 1

Ion conductivity σ and pH data of filtrates obtained at different stages of functionalised hBN particle washing

PDDA Amount (wt%)	Filtrate No. 1		Filtrate No. 2		Filtrate No. 3	
	σ (μS/cm)	pH	σ (μS/cm)	pH	σ (μS/cm)	pH
0.3	22.1	5.65	7.12	5.27	2.08	4.87
0.4	26.9	5.45	10.09	5.52	2.36	4.41
0.5	24.9	5.11	8.03	5.39	1.43	4.78
0.6	26.1	5.30	8.55	5.44	2.23	6.25

The filtrates collected from the second and third washes exhibited substantial decreases in conductivity and even fell below the 13 μS/m baselines set by the as-received hBN washing filtrate [Figure 3(b)]. The conductivities of the filtrates after the second and third washes declined to 8.4 and 2.0 μS/m, respectively. The filtrates also recorded slightly reduced pH readings as the number of washes increased (Table 1), indicating that the filtrate had become increasingly acidic. The decrement in the pH of the PDDA-functionalised

suspensioncaused the reduction in zeta potential (Zarbov et al., 2004). Low zeta potential strengthens attraction between suspension particles, thus increasing the possibility of particle agglomeration (Moreno, 2020).

The particle size range broadened after the completion of the third water washing cycle of the functionalised particles [Figure 4(b)]. The minimum particle size decreased from 0.3 µmto 0.2 µm, and the volume of particle sizes over 20 µm increased to more than 2.5 vol%. Nevertheless, the volume percentage of particles smaller than 1.5 µm had drastically reducedto below 4 vol% with the particle size distribution expanding towards large size values. Functionalised particles appeared to be larger than nonfunctionalised particles, indicating thatparticle agglomeration was caused by PDDA functionalisation. Comparing the particle size distribution of the functionalised [Figure 4(b)] and nonfunctionalised particles [Figure 4(a)] revealed that the percentage of functionalised particles involved in particle agglomeration was higher than that of the deagglomerated as-received particles.

Suspension Stability Data

The sedimentation test data indicated that the washed and nonwashed functionalised hBN particles displayed contrasting particle stability behaviours with the increase in PDDA content (Figures 5 & 6). The washed particle group exhibited a reduction in suspension stability with the increase in PDDA content. Meanwhile, the nonwashed particle group displayed a slight increase with the increase in PDDA content. Furthermore, the comparison of the total height of sedimentation data (Figure 6) revealed the considerably lower particle suspension stability of the washed particles than that of the nonwashed particles at a similar PDDA content. The discrepancy between the data of the washed and nonwashed groups demonstrated the strong influence of the ion impurities released from the nonwashed hBN particles on the increase in the suspension stability of the hBN particles. Conductivity [Figure 3(b)] and particle size data [Figures 4(a) & (b)] suggested that the reduction in the suspension stability of the washed particles was due to particle agglomeration caused by the lowered zeta potential largely because the ion impurities were mostly removed from the hBN particles through washing prior to functionalisation. Figure 3 illustrates that the ion conductivity of the PDDA-functionalised hBN particles before washing was lower (approximately 25 µS/cm) than that of the as-received hBN particles before washing (180 µS/cm).

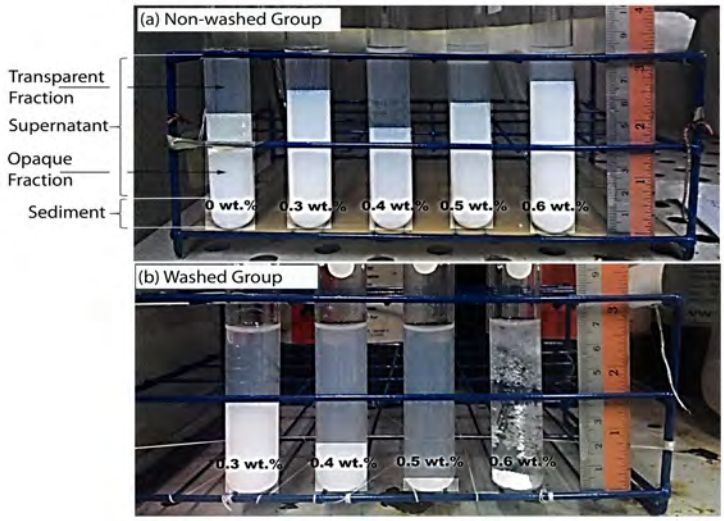

Figure 5. Qualitative sedimentation results of the hBN particle suspensions functionalised with different PDDA contents (wt% of hBN basis) on the 14th day after agitation: (a) nonwashed and (b) washed sample groups. Here, 0 wt% (controlled) suspension was prepared using the as-received hBN particles

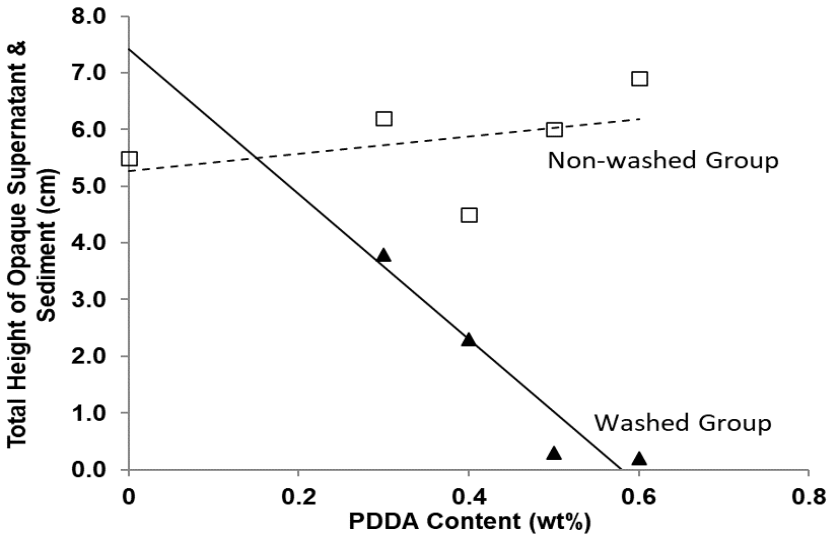

Figure 6. Quantitative sedimentation results plotted against the PDDA content of (a) nonwashed and (b) washed groups

The change in the influence of PDDA on suspension stability from weak to strong after the removal of the ion impurities clearly illustrated a shift from an ion-driven stabilisation mechanism to a PDDA-driven particle agglomeration mechanism. This shift was reflected by the reduction in the suspension stability of the washed particles with the increase in PDDA content. However, the formation of dense sediments by the 0.5 wt% and 0.6 wt%

suspensions indicated a compact particle arrangement. This result suggested that strong interparticle bonding between particles occurred only through PDDA cross-linking. Cross-links between PDDA form through amine groups (Du et al., 2020).

The agglomeration of the PDDA-functionalised particles was driven by the cross-linking of PDDA between the PDDA-functionalised hBN particles when dispersed in a suspension with an extremely low ion concentration (~2 µS/cm). The strong pull of gravity on the heavy particle agglomerates resulted in the low stability of the hBN particle suspension. High PDDA contents implied a high degree of the surface functionalisation of hBN particles, indicating increased cross-linking between the functionalised suspension particles. This phenomenon was demonstrated only when free ions were eliminated with the usage of DI water and through the repeated water washing of the functionalised hBN particles. As the surface coverage of the hBN particles with PDDA increased with the increase in PDDA content, PDDA cross-linking became increasingly likely, resulting in the reduced suspension stability of the PDDA-functionalised hBN particles.

Electric double-layer (EDL) theory is used to explain the suspension stability mechanism of polyelectrolyte-functionalised colloidal particles (Moreno, 2020). In the presence of a significant concentration of free ions in the nonwashed suspension, an EDL formed around the PDDA chains of the functionalised hBN particles, thus creating PDDA with stretched conformation (Lewis, 2000). PDDA exhibits strong anion adsorption via amine group attraction (Du et al., 2020; Turhan & Bicak, 2020). Steric stabilisation between the PDDA- functionalised particles prevented cross-linking between PDDA in the suspension with a highion concentration (above 20 µS/cm). The addition of PDDA to the nonwashed suspension resulted in a slight increase in suspension stability driven by the improved steric stabilisation mechanism (Lau & Sorrell, 2011).

hBN Deposit Yield, Raman and SEM Micrograph Data

The plot of the hBN deposition yields of the washed and nonwashed particles as a function ofPDDA content followed the linear Hamaker's law. Hamaker's law expresses the relationship between deposition yield $m(t)$ and the EPD parameters (Kinzl et al., 2009) as Equation 1:

$$m(t) = \int_0^t f \cdot M_E \cdot A \cdot c(t) \cdot E(t) \cdot \mathrm{d}t \qquad [1]$$

where

t is deposit time in s,

f is the unitless efficiency factor ($0 \leq f \leq 1$; $f = 1$ if all particles that reached the substrate aredeposited),

M_E is the electrophoretic mobility in µm.cm/V.s,

A is the deposited surface area in cm^2,
$c(t)$ is the particle mass concentration in grams and
$E(t)$ is the applied electric field in V/cm.

In this study, all the EPD parameters, except the electrophoretic mobility of the hBN particles, were fixed. Electrophoretic mobility was presumed to be determined predominantly by the electrophoretic response of the PDDA that had attached to the hBN particles. Previously, PDDA addition had a positive and linear correlation with electrophoretic mobility (Lau & Sorrell, 2011). The increase in PDDA addition amount likely contributed to the linear increase in the electrophoretic mobility of PDDA-functionalised hBN particles and consequently gave rise to a linear increase in the deposition yield (Figure 7).

However, the deposition yields of the washed and nonwashed particles showed an obvious discrepancy. Specifically, the washed particles had higher hBN deposition yields than the nonwashed particles (Figure 7). The yield data were verified on the basis of Raman spectra (Figure 8). The single hBN peak intensity at 1357 cm^{-1} detected on the deposits produced by the washed group was higher than that of the deposits produced by the nonwashed group. At the same time, the hBN peak intensity for the EPD suspension also increased with the increase in PDDA content. Previous studies had attributed the increment inpeak intensity to the increase in hBN thickness (Cao et al., 2014; Zhou et al., 2014).

Furthermore, the hBN particle deposits produced by the washed and nonwashed particles with different PDDA contents maintained their Raman peak position at the same Raman shiftfrequency. The Raman data implied that the crystallinity and exfoliation degree of the functionalised hBN particles deposited on the GI substrate remained unchanged after washing or functionalisation (Cao et al., 2014; Zhou et al., 2014).

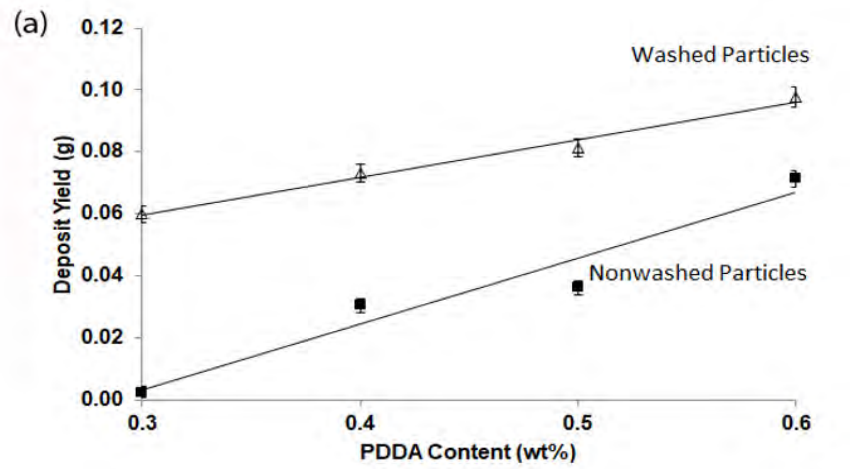

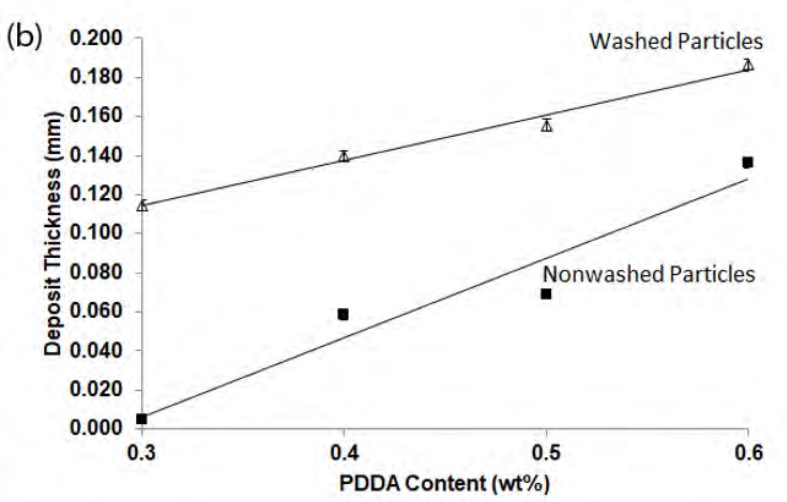

Figure 7. (a) Deposition yield and (b) calculated deposition thickness versus PDDA content obtained by EPD using functionalised hBN particles from the nonwashed and washed groups

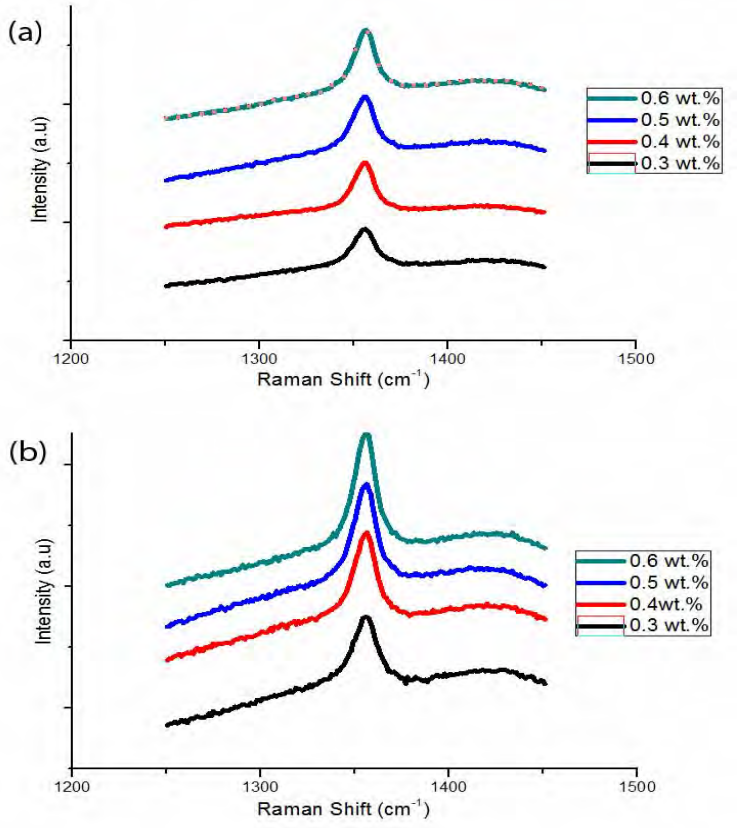

Figure 8. Raman spectra versus the PDDA content of the hBN deposits produced through EPD using functionalised particles from the: (a) nonwashed and (b) washed groups

This work argued that the washing of PDDA-functionalised hBN particles increased the deposition efficiency factor (Equation 1) of the washed hBN particles to a value that was significantly higher than that of the nonwashed particles. Although the washed group displayed lower suspension stability (Figures 5 & 6), the EPD yield [Figure 7(a)] of this group was higher than that of the nonwashed group at the same PDDA content. The removal of free ions (i.e., ion impurities) from the functionalised hBN particles by washing reduced thethickness of the EDL surrounding the hBN particles. Particle agglomerates formed in the suspension (as discussed in the earlier section) as the cross-linking between the PDDA-functionalised particles became increasingly dominant with the increase in PDDA content. Lowsuspension particle stability facilitated particle deposition (i.e., increased efficiency) and resulted in high EPD yields. The deposited hBN particles showed signs of particle agglomeration during EPD, as shown in Figures 9 and 10. The washed and nonwashed groupsformed uneven deposits in which the deposited particles showed signs of particle agglomeration. Nearly all deposited particles had particle sizes of less than 1 μm, implying that only particle-agglomeration-driven deposition affected colloidal-sized particles. The deposited particles had had highly spherical shapes (Figure 10) in contrast to the as-received particles that had poorly spherical shapes (Figure 1). This result indicated that particle functionalisation also caused a change in particle shape through particle agglomeration.

The deposition yield of washed particles increased linearly with the increase in PDDA, and the yield variation of the nonwashed group narrowed gradually from 183% to 31% [Figure 7(a)]. The improved EPD yield performance of the nonwashed and washed groups at high PDDA content demonstrated the positive effect of PDDA addition on the EPD of hBN particles. Nevertheless, EPD using high PDDA contents resulted in considerable variances in deposition yields because particle agglomeration drove deposition instability. Finally, this study demonstrated that the high EPD yield of the PDDA-functionalised hBN particles could be achieved by controlling the ion concentration of the EPD suspension to an extremely low level (i.e., 2 μS/cm) by eliminating the free ions that had leached from the suspended hBN particles via the repeated water washing of the particles immediately before and after PDDA functionalisation. This work also believed that the surface microstructure of EPD deposits became increasingly even and dense with the increase in deposition time and applied voltage because the deposition pressure imposed by the incoming deposited particles caused particle rearrangement. Under the assumption that the porosity of the EPD coating was negligible anddeposition thickness was even throughout the deposition area, the estimated deposition thickness *t* was calculated r the following Equation 2:

$$t = \frac{m}{A\rho} \qquad [2]$$

where
m is the deposit yield in grams,
A is the deposition area in mm^2 and
ρ is the density of hBN, which is 2.2 g/cm^2 (Yu et al., 2021).

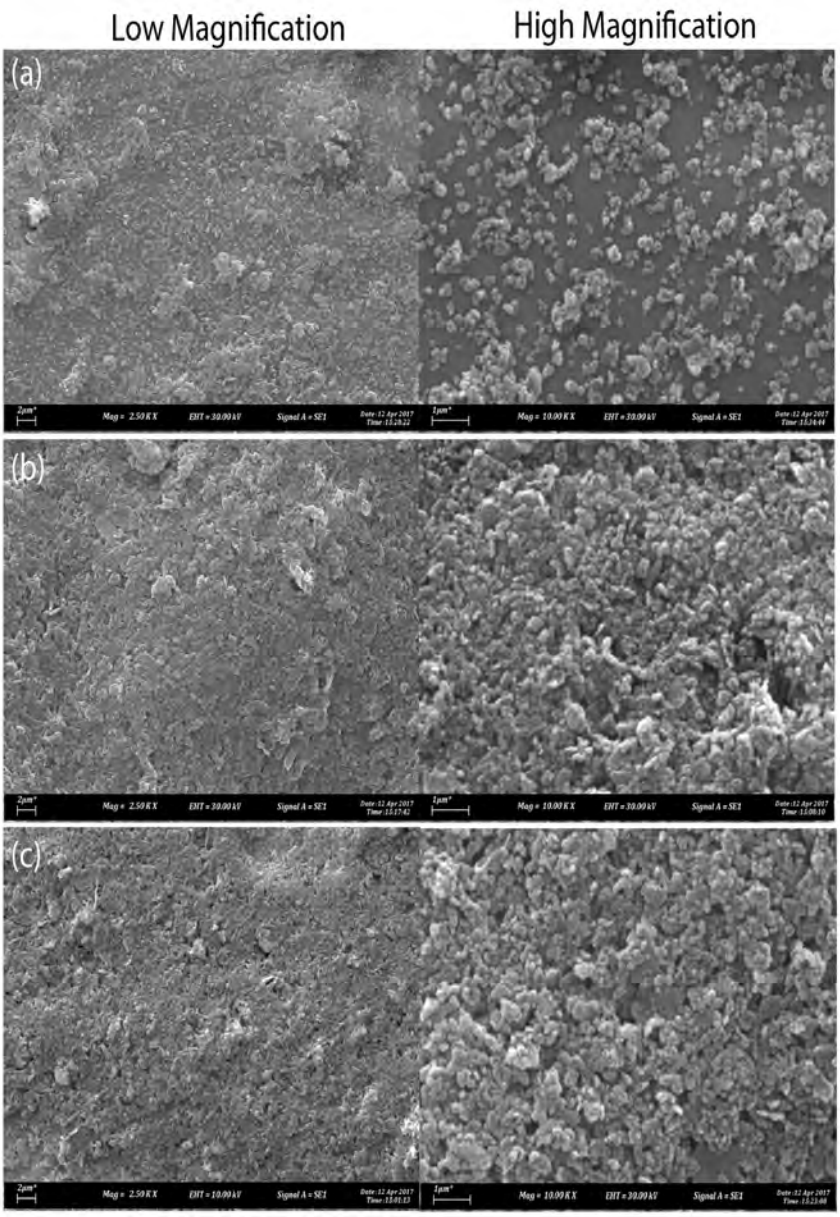

Figure 9. SEM micrographs of the surface microstructures of the hBN deposits produced using hBN particles functionalised with 0.6 wt% PDDA from the (a) nonwashed and (b) washed groups. Deposits were obtained using particles functionalised with 0.3 wt% PDDA from the washed group (c) are presented for comparison

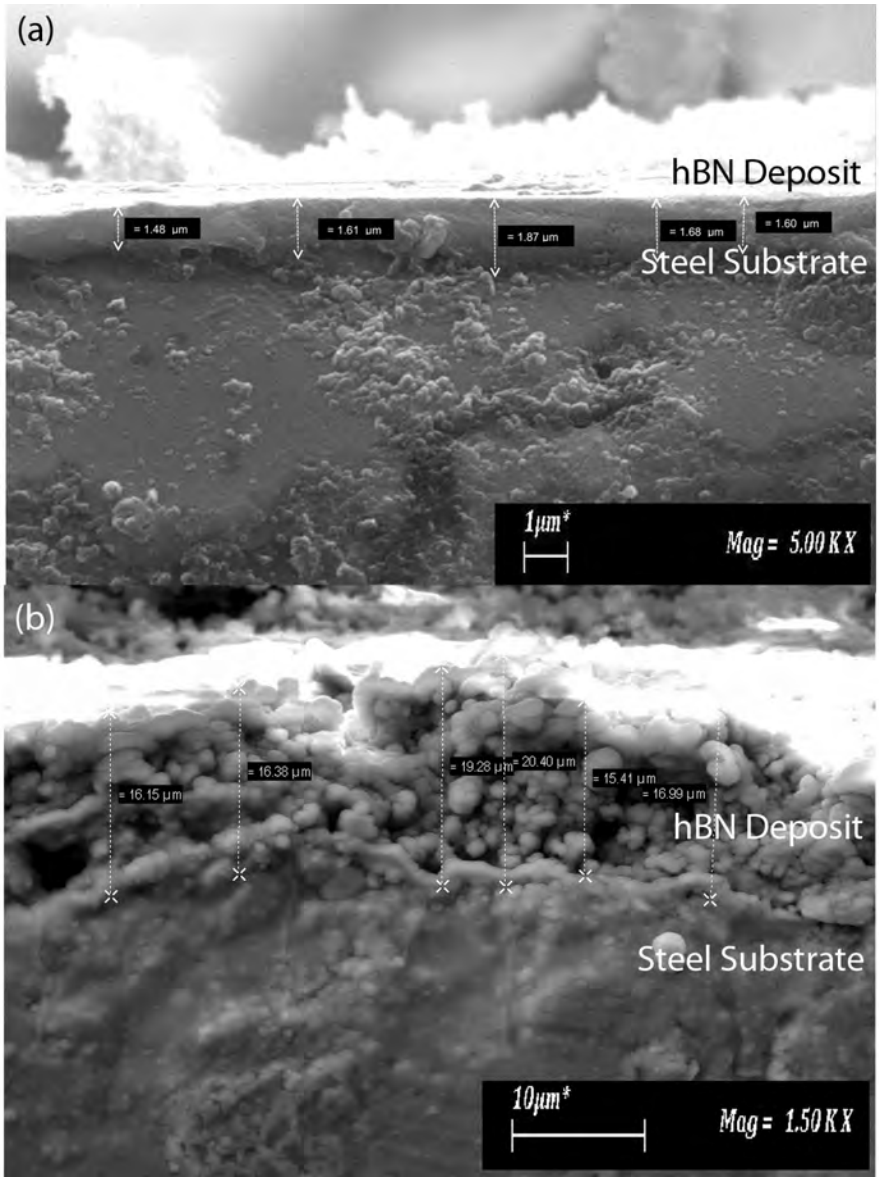

Figure 10. SEM micrographs of the cross-sectional microstructures of hBN deposits produced using particles functionalised with 0.6 wt% PDDA from the (a) nonwashed and (b) washed groups

Figure 7(b) shows the calculated deposition thickness plotted as a function of PDDA content. The plot shows that the EPD of washed particles yielded a deposition thickness of 115 µm, whereas particles functionalised with a low PDDA content (0.3 wt%) were 5 µm. Thedeposition thickness of the washed particles had exceeded the minimum thickness thresholdof 20 µm that corresponded to the equivalent dielectric breakdown strength of 4.5 kV/s. Theequivalent dielectric breakdown strength of 10 kV/s, which is the minimum electrical isolation requirement for high-voltage transistor packages, may be obtained at the thickness of 100–300 µm when combined with a polymer binder (Lau & Narayanasamy, 2018). Although the deposition thicknesses of the washed and nonwashed particles increased to 187 and 136 µm, respectively, as the PDDA content was increased to 6 wt%, the use of low PDDA contents is sustainable because it minimises electrolytic corrosion and chemical nonequilibrium risks.

CONCLUSION

This work reported the effect of hBN particle washing and PDDA functionalisation on hBN particle suspension stability and EPD yield. The repeated washing procedure performed on the as-received and PDDA-functionalised hBN particles successfully eliminated the interference of free ions on the influence of PDDA on hBN particle suspension stability and EPD yield. The ion concentration of the PDDA-functionalised hBN particle suspension was controlled at ~2 µS/cm. As a result, the suspension stability of the PDDA-functionalised hBN particles decreased linearly as the PDDA content was increased from 0.3 wt% to 0.6 wt%. In contrast, the EPD yield of the hBN particles increased linearly with the increment to the samePDDA wt%. The reduction in suspension stability with the increase in PDDA content was hypothesised to be due to the increased agglomeration of PDDA-functionalised hBN particles through PDDA cross-linking. The decreased suspension stability of the PDDA-functionalised particles resulted in the increased deposition yield of colloidal-sized hBN particles. Future works should conduct zeta potential and surface analyses on functionalised hBN particles to understand further PDDA functionalisation and its interactions in aqueous suspensions with ultralow ion concentrations.

ACKNOWLEDGEMENTS

The authors would like to acknowledge Universiti Teknikal Malaysia Melaka (UTeM) for the sample preparation and characterisation facilities. Portions of this research were done while the authors were in the Faculty of Manufacturing Engineering, UTeM. Special thanks to Azhar Shah, Hairulhisham and Mohd Farihan of Faculty of Manufacturing Engineering, UTeM for the technical support in SEM, Particle Size Analyser, and Raman characterisations.

REFERENCES

Bandara, Y. W., Gamage, P., & Gunarathne, D. S. (2020). Hot water washing of rice husk for ash removal: The effect of washing temperature, washing time and particle size. *Renewable Energy, 153*, 646-652. https://doi.org/10.1016/j.renene.2020.02.038

Cao, L., Emami, S., & Lafdi, K. (2014). Large-scale exfoliation of hexagonal boron nitride nanosheets in liquid phase. *Materials Express, 4*(2), 165-171. https://doi.org/10.1166/mex.2014.1155

Cui, M., Njoku, D. I., Li, B., Yang, L., Wang, Z., Hou, B., & Li, Y. (2021). Corrosion protection of aluminium alloy 2024 through an epoxy coating embedded with smart microcapsules: The responses of smart microcapsules to corrosive entities. *Corrosion Communications, 1*, 1-9. https://doi.org/10.1016/j.corcom.2021.06.001

Du, X., Zhang, H., Yuan, Y., & Wang, Z. (2020). Semi-interpenetrating network anion exchange membranes based on quaternized polyvinyl alcohol/poly (diallyldimethylammonium chloride). *Green Energy & Environment, 6*(5), 743-750. https://doi.org/10.1016/j.gee.2020.06.015

Ertuğ, B. (2013). Powder preparation, properties and industrial applications of hexagonal boron nitride. In *Sintering Applications* (pp. 33-54). IntechOpen. https://doi.org/10.5772/53325

Gautam, P., Bajagain, R., & Jeong, S. W. (2020). Combined effects of soil particle size with washing time and soil-to-water ratio on removal of total petroleum hydrocarbon from fuel contaminated soil. *Chemosphere, 250*, Article 126206. https://doi.org/10.1016/j.chemosphere.2020.126206

Hafeez, A., Karim, Z. A., Ismail, A. F., Samavati, A., Said, K. A. M., & Selambakkannu, S. (2020). Functionalized boron nitride composite ultrafiltration membrane for dye removal from aqueous solution. *Journal of Membrane Science, 612*, Article 118473. https://doi.org/10.1016/j.memsci.2020.118473

Ihsanullah, I. (2020). Boron nitride-based materials for water purification: Progress and outlook. *Chemosphere, 263*, Article 127970. https://doi.org/10.1016/j.chemosphere.2020.127970

Katagiri, K., Uemura, K., Uesugi, R., Inumaru, K., Seki, T., & Takeoka, Y. (2018). Structurally colored coating films with tunable iridescence fabricated via cathodic electrophoretic deposition of silica particles. *RSC Advances, 8*(20), 10776-10784. https://doi.org/10.1039/c8ra01215f

Khalaj, M., Golkhatmi, S. Z., Alem, S. A. A., Baghchesaraee, K., Azar, M. H., & Angizi, S. (2020). Recent progress in the study of thermal properties and tribological behaviors of hexagonal boron nitride-reinforced composites. *Journal of Composites Science, 4*(3), Article 116. https://doi.org/10.3390/jcs4030116

Kinzl, M., Reichmann, K., & Andrejs, L. (2009). Electrophoretic deposition of silver from organic PDADMAC-stabilized suspensions. *Journal of Materials Science, 44*(14), 3758-3763. http://dx.doi.org/10.1007/s10853-009-3504-x

Lalau, C. C., & Low, C. T. J. (2019). Electrophoretic deposition for lithium-ion battery electrode manufacture. *Batteries & Supercaps, 2*(6), 551-559. https://doi.org/10.1021/acsami.7b10683.s001

Lau, K. T., & Narayanasamy, J. (2018). Semiconductor component and method for producing a semiconductor component. *US Patent, US 10,121,723 B1*.

Lau, K. T., & Sorrell, C. C. (2011). Electrophoretic mobilities of dissolved polyelectrolyte charging agent and suspended non-colloidal titanium during electrophoretic deposition. *Materials Science and Engineering: B, 176*(5), 369-381. https://doi.org/10.1016/j.mseb.2010.10.012

Lau, K. T., & Sorrell, C. C. (2013). Effect of charging agents on electrophoretic deposition of titanium particles. *Journal of The Australian Ceramic Society, 49*(2), 104-112.

Lewis, J. A. (2000). Colloidal processing of ceramics. *Journal of the American Ceramic Society, 83*(10), 2341-2359.

Li, J., Hao, L., Zheng, F., Chen, X., Wang, S., & Fan, Y. (2020). Erosion corrosion behavior of aluminum electrode in simulated HVDC water cooling at 50°C. *International Journal of Electrochemical Science, 15*, 5320-5332. https://doi.org/10.1002/maco.202112453

Lin, Z F., Wang, Y., Zhang, D., & Li, X. B. (2016). Corrosion resistance research of ZnO/polyelectrolyte composite film. *International Journal of Electrochemical Science, 11*, 8512-8519. https://doi.org/10.20964/2016.10.37

Moreno, R. (2020). Better ceramics through colloid chemistry. *Journal of the European Ceramic Society, 40*(3), 559-587. https://doi.org/10.1016/j.jeurceramsoc.2019.10.014

Muto, H., Yokoi, A., & Tan, W. K. (2020). Electrostatic assembly technique for novel composites fabrication. *Journal of Composites Science, 4*(4), Article 155. https://doi.org/10.3390/jcs4040155

Narayanasamy, J., Lau, K. T., & Zaimi, M. (2016). Transistor package's boron nitride film microstructure and roughness: Effect of EPD suspensions' pH and binder. *Journal of Telecommunication, Electronic and Computer Engineering (JTEC), 8*(2), 99-104.

Nasser, J., Steinke, K., Zhang, L., & Sodano, H. (2020). Enhanced interfacial strength of hierarchical fiberglass composites through an aramid nanofiber interphase. *Composites Science and Technology, 192*, Article 108109. https://doi.org/10.1016/j.compscitech.2020.108109

Sanchez, J. S., Xu, J., Xia, Z., Sun, J., Asp, L. E., & Palermo, V. (2021). Electrophoretic coating of $LiFePO_4$/graphene oxide on carbon fibers as cathode electrodes for structural lithium ion batteries. *Composites Science and Technology, 208*, Article 108768. https://doi.org/10.1016/j.compscitech.2021.108768

Tiwari, P., Ferson, N. D., & Andrew, J. S. (2020). Elucidating the role of electrophoretic mobility for increasing yield in the electrophoretic deposition of nanomaterials. *Journal of Colloid and Interface Science, 570*, 109-115. https://doi.org/10.1016/j.jcis.2020.02.103

Turhan, H., & Bicak, N. (2020). Selective dinitramide removal from aqueous solution by crosslinked polyDADMAC gels. *Propellants, Explosives, Pyrotechnics, 45*(6), 981-987. https://doi.org/10.1002/prep.201900271

Yu, K., Yuan, T., Zhang, S., & Bao, C. (2021). Hypergravity-induced accumulation: A new, efficient, and simple strategy to improve the thermal conductivity of boron nitride filled polymer composites. *Polymers, 13*(3), Article 459. https://doi.org/10.3390/polym13030459

Zarbov, M., Schuster, I., & Gal-Or, L. (2004). Methodology for selection of charging agents for electrophoretic deposition of ceramic particles. *Journal of Materials Science, 39*(3), 813-817.

Zhou, H., Zhu, J., Liu, Z., Yan, Z., Fan, X., Lin, J., Wang, G., Yan, Q., Yu, T., Ajayan, P. M., & Tour, J. M. (2014). High thermal conductivity of suspended few-layer hexagonal boron nitride sheets. *Nano Research, 7*(8), 1232-1240. https://doi.org/10.1007/s12274-014-0486-z